Inorganic Chemistry Article

Inorg. Chem. **2009,** *48,* 4971–4979 **4971**
DOI:10.1021/ic900292h

Zn_3, Ni_3, and Cu_3 Complexes of a Novel Tricompartmental Acyclic Ligand

Matilde Fondo,[*,†] **Noelia Ocampo,**[†] **Ana M. García-Deibe,**[†] **and Jesús Sanmartín**[‡]

[†]*Departamento de Química Inorgánica, Facultade de Ciencias, Universidade de Santiago de Compostela, 27002 Lugo, Spain, and* [‡]*Departamento de Química Inorgánica, Facultade de Química, Universidade de Santiago de Compostela, 15782 Santiago de Compostela, Spain*

Received February 13, 2009

A new tricompartmental acyclic ligand (H_4L) was prepared and fully characterized. It reacts with zinc, nickel, and copper(II) acetate to yield $[Zn_3L(OAc)_2]\cdot H_2O$ (**1**$\cdot H_2O$), $[Ni_3L(OAc)_2(MeOH)_2]\cdot 2MeCN\cdot 2MeOH$ (**2**$\cdot$2MeCN$\cdot$2 MeOH), and $[Cu_3L(OAc)_2]\cdot 3H_2O$ (**3**$\cdot 3H_2O$), respectively. **2**$\cdot$2MeCN$\cdot$2MeOH precipitates as single crystals, which lose the solvates upon drying to give **2**. The reactivity of the acetate complexes in a methanol/acetonitrile basic medium in air was investigated. Thus, **1**$\cdot H_2O$ and **2** are unstable in this medium, both suffering partial hydrolysis to produce single crystals of $[Zn_3L(3\text{-Br-5-Cl-Sal})_2]\cdot 2MeCN$ (**4**$\cdot$2MeCN; 3-Br-5-Cl-Sal$^-$ = 3-bromo-5-chlorosalicylaldehydate) and $[Ni_3L(3\text{-Br-5-Cl-Sal})_2]\cdot 2MeCN$ (**5**$\cdot$2MeCN) as one of the reaction byproducts, while **3**$\cdot 3H_2O$ gives rise to a reaction of ligand displacement, generating crystals of $[Cu_3L(OMe)_2]\cdot MeOH$ (**6**$\cdot$MeOH). Complexes **2**$\cdot$2MeCN$\cdot$2MeOH, **4**$\cdot$2MeCN, **5**$\cdot$2MeCN, and **6**$\cdot$MeOH were crystallographically characterized, and these studies demonstrate not only the trinucleating ability of the fully deprotonated L^{4-} ligand but also its tendency to induce chirality in the isolated compounds. The magnetic characterization of **2**, **3**$\cdot 3H_2O$ and **6**$\cdot$MeOH shows that the magnetic coupling between adjacent metal ions is weak, with **2** being ferromagnetic and **3**$\cdot 3H_2O$ and **6**$\cdot$MeOH antiferromagnetic.

Introduction

Since Robson's seminal papers published in 1970,[1] many either acyclic or macrocyclic dinucleating compartmental ligands (i.e., ligands with two chambers in close proximity that provide at least one endogenous bridge)[2] have been synthesized, most of them coming from the symmetrical dialdehyde 2,6-diformylphenol.[3,4] One of the interesting features of this kind of ligand is that the nature of the donor atoms, as well as the distance between them, can be varied fairly simple, and this can substantially modify the properties of their complexes. Thus, these ligands may be designed to generate homo- or heterodinuclear complexes with specific magnetic or optical properties, or they can form complexes that are efficient catalysts in many processes of industrial or biological relevance.[3,4] In addition, these dinuclear compounds can be used as nodes in the obtainment of polynuclear complexes and/or coordination polymers.[5]

In spite of the rich and promising chemistry of dicompartmental donors, the synthesis of tricompartmental ligands and the study of its chemistry are nowadays much less explored.[6−11] As far as we know, among these potential tricompartmental ligands, many of them are macrocycle donors that really act as dinucleating ligands, leading to dinuclear complexes.[6,7] Thus, to the best of our knowledge, the tricompartmental acyclic ligands and its coordination chemistry are research fields that are still quite scarcely investigated.

---

[*] To whom correspondence should be addressed. E-mail: matilde.fondo@usc.es.

[1] (a) Robson, R. *Inorg. Nucl. Chem. Lett.* **1970**, *6*, 125–128. (b) Robson, R. *Aust. J. Chem.* **1970**, *23*, 2217–2224. (c) Pilkington, N. H.; Robson, R. *Aust. J. Chem.* **1970**, *23*, 2225–2236.

[2] Guerreiro, P; Vigato, P. A; Zanello, P.; Garziani, R. *Inorg. Chim. Acta* **1988**, *141*, 103–118.

[3] Vigato, P. A.; Tamburini, S.; Bertolo, L. *Coord. Chem. Rev.* **2007**, *251*, 1311–1492 and references cited therein.

[4] Vigato, P. A.; Tamburini, S. *Coord. Chem. Rev.* **2008**, *252*, 1871–1995 and references cited therein.

[5] Andruh, M. *Chem. Commun.* **2007**, 2565–2577.

[6] (a) Akilan, P.; Thirumavalavan, M.; Kandaswamy, M. *Polyhedron* **2003**, *22*, 1407–1413. (b) Thirumavalavan, M.; Akilan, P.; Kandaswamy, M.; Kandaswamy, C.; Kumar, G. S. *Inorg. Chem.* **2003**, *42*, 3308–3317. (c) Thirumavalavan, M.; Akilan, P.; Kandaswamy, M. *Supramol. Chem.* **2004**, *16*, 495–504. (d) Thirumavalavan, M.; Akilan, P.; Kandaswamy, M. *Polyhedron* **2006**, *25*, 2623–2628.

[7] Salmon, L.; Thuéry, P.; Rivière, E.; Miyamoto, S.; Yamato, T.; Ephritkhine, M. *New J. Chem.* **2006**, 1220–1227.

[8] Glaser, T.; Liratzis, I.; Fröhlich, R.; Weyhermüller, T. *Chem. Commun.* **2007**, 356–358.

[9] Akine, S.; Taniguchi, T.; Nabeshima, T. *J. Am. Chem. Soc.* **2006**, *128*, 15765–15774.

[10] Shiga, T.; Ohba, M.; Okawa, H. *Inorg. Chem.* **2004**, *43*, 4435–4446.

[11] (a) Saalfrank, R. W.; Seitz, V.; Caulder, D. L.; Raymond, K. N.; Teichert, M.; Stalke, D. *Eur. J. Inorg. Chem.* **1998**, 1313–1317. (b) Saalfrank, R. W.; Seitz, V.; Heinemann, F. W.; Göbel, C.; Herbst-Irmer, R. *J. Chem. Soc., Dalton Trans.* **2001**, 599–603.

Scheme 1

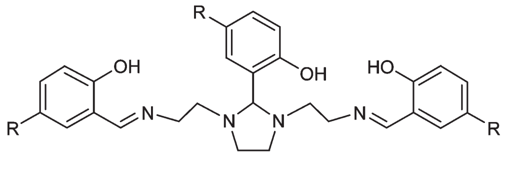

H_3L^x

Scheme 2. Synthesis of H_4L, with a Numbering Scheme for NMR Spectroscopy

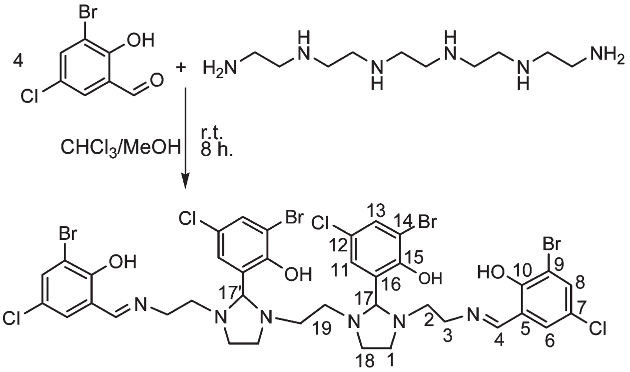

During the last years, we have been working with a particular type of dicompartmental acyclic ligand (Scheme 1),[12] based on Schiff's condensation of tetraethylenetetramine and different aldehydes. This kind of donor shows some outstanding features and, accordingly, we could successfully demonstrate that it favors ferromagnetic coupling because of its ability to provide an $NCN_{imidazolidine}$ bridge between the metal atoms allocated in its compartments.[12c] Besides, many complexes with this type of donor spontaneously fix carbon dioxide from air, converting it into carbonato.[12a−12d] In addition, its homodinuclear complexes can act as building blocks in the isolation of tetranuclear compounds,[12] some of which show remarkable magnetic properties.[12c,12d]

With these previous results in mind, we tried to enlarge this type of ligand into trinucleating systems by increasing the number of amino groups of the amine reactant. Thus, in this work, a novel tricompartmental acyclic ligand (H_4L, Scheme 2), derived from pentaethylenehexamine, is reported and its reactivity toward zinc(II), nickel(II), and copper(II) analyzed.

Experimental Section

General Considerations. Elemental analyses of C, H, and N were performed on a Carlo Erba EA 1108 analyzer. IR spectra were recorded as KBr pellets on a FT-IR Bruker IFS-66v spectrophotometer in the range 4000−400 cm^{-1}. The fast atom bombardment (FAB) mass spectrum of H_4L was recorded on an AUTOSPEC spectrometer, using *m*-nitrobenzylalcohol (MNBA) as a matrix. Electrospray (ES) mass spectra of the metal complexes were obtained on a Hewlett-Packard LC/MS spectrometer, with methanol as the solvent. ^1H NMR spectra were recorded on a Bruker AMX500 spectrometer, using deuterated dimethyl sulfoxide (DMSO-d_6) as the solvent.

Syntheses. All solvents, 3-bromo-5-chlorosalicylaldehyde (3-Br-5-Cl-Sal), pentaethylenehexamine, $Zn(OAc)_2\cdot 2H_2O$, $Ni(OAc)_2\cdot 4H_2O$, $Cu(OAc)_2\cdot H_2O$, and tetramethylammonium hydroxide pentahydrate, are commercially available and were used without further purification.

H_4L. 3-Br-5-Cl-Sal (0.595 g, 2.53 mmol) and 15 mL of methanol were added to a chloroform solution (~5 mL) of pentaethylenehexamine (0.147 g, 0.63 mmol) at room temperature. The mixture was stirred in air for 8 h, precipitating a yellow solid. The solid was filtered off, washed with diethyl ether, and dried in air (0.38 g, 55%). Mp: 190−192 °C. Calcd for $C_{38}H_{36}Br_4Cl_4N_6O_4$ (1102.0): C, 41.38; H, 3.27; N, 7.62. Found: C, 41.34; H, 3.33; N, 7.52. MS (FAB): *m/z* 1102.8 $[H_5L]^+$. IR (KBr, ν/cm^{-1}): 1636 (C=N), 3437 (OH). ^1H NMR (500 MHz, DMSO-d_6): δ 2.27−2.39, 2.40−2.49, 2.54−2.76, 2.76−2.89, 2.90−3.07, 3.57−3.64 (all m, 20H, 4H1 + 4H2 + 4H3 + 4H18 + 4H19), 3.80, 3.94 (both s, 1H each, H17 + H17′), 7.15, 7.38, 7.49, 7.67 (all s, 2H each, 2H6 + 2H8 + 2H11 + 2H13), 8.36 (s, 2H, 2H4), 12.02 (broad, 2H, OH), 14.30 (broad, 2H, OH).

$[Zn_3L(OAc)_2]\cdot H_2O$ ($1\cdot H_2O$). To a methanol/acetonitrile (20/20 mL) solution of $Zn(OAc)_2\cdot 2H_2O$ (0.12 g, 0.55 mmol) was added H_4L (0.20 g, 0.18 mmol). The mixture was stirred in air at room temperature for 6 h, and the resultant solution was left to slowly evaporate until a yellow solid precipitated. The solid was filtered off and dried in air (0.108 g, 42%). Mp: > 300 °C. Calcd for $C_{42}H_{40}Br_4Cl_4N_6O_9Zn_3$ (1430.20): C, 35.20; H, 2.79; N, 5.87. Found: C, 34.98; H, 2.93; N, 5.99. MS (ES^+): *m/z* 1310.4 $[Zn_3L(OH)]^+$; 1354.4 $[Zn_3L(OAc)]^+$. IR (KBr, ν/cm^{-1}): 1632 (C=N), 3429 (H_2O). ^1H NMR (500 MHz, DMSO-d_6): δ 1.80 (s, 6H, OAc), 2.22−2.37, 2.38−2.47, 2.50−2.76, 2.78−2.95, 3.46−3.63, 3.67−3.83 (all m, 20H, 4H1 + 4H2 + 4H3 + 4H18 + 4H19), 4.01, 4.61 (both s, 1H each, H17 + H17′), 7.22−7.40, 7.55−7.65 (both m, 8H, 2H6 + 2H8 + 2H11 + 2H13), 8.36 (s, 2H, 2H4).

$[Ni_3L(OAc)_2(MeOH)_2]$ (2). $\mathbf{2}\cdot 2MeCN\cdot 2MeOH$ was obtained as green single crystals by the same method as that of $\mathbf{1}\cdot H_2O$. The crystals were filtered off and dried in air (0.10 g, 39%). Mp: > 300 °C. The elemental analysis is in agreement with the proposed formulation **2**, showing that the crystals lose the solvates upon drying. Calcd for $C_{43}H_{42}Br_4Cl_4N_6Ni_3O_9$ (1456.70): C, 36.25; H, 3.16; N, 5.77. Found: C, 36.10; H, 2.94; N, 5.80. MS (ES^+): *m/z* 1290.6 $[Ni_3L(OH)]^+$, 1332.6 $[Ni_3L(OAc)]^+$. IR (KBr, ν/cm^{-1}): 1634 (C=N).

$[Cu_3L(OAc)_2]\cdot 3H_2O$ ($3\cdot 3H_2O$). This complex is obtained by the same method as that of $\mathbf{1}\cdot H_2O$, from $Cu(OAc)_2\cdot H_2O$ (0.10 g, 0.48 mmol) and H_4L (0.18 g, 0.16 mmol). Yield: 0.10 g (43%). Mp: > 300 °C. Calcd for $C_{42}H_{44}Br_4Cl_4Cu_3N_6O_{11}$ (1460.6): C, 34.51; H, 3.01; N, 5.75. Found: C, 34.59; H, 2.85; N, 5.67. MS (ES^+): *m/z* 1305.6 $[Cu_3L(OH)]^+$, 1347.6 $[Cu_3L(OAc)]^+$. IR (KBr, ν/cm^{-1}): 1628 (C=N), 3423 (H_2O).

$[Zn_3L(3\text{-}Br\text{-}5\text{-}Cl\text{-}Sal)_2]\cdot 2MeCN$ ($4\cdot 2MeCN$). To a methanol/acetonitrile (20/20 mL) suspension of $\mathbf{1}\cdot H_2O$ (0.05 g, 0.036 mmol) was added $NMe_4OH\cdot 5H_2O$ (0.013 g, 0.072 mmol). The mixture was stirred in air at room temperature for 6 h, and the resultant solution was left to slowly evaporate (4 weeks) until a few crystals of $\mathbf{4}\cdot 2MeCN$, suitable for X-ray diffraction studies, precipitated.

$[Ni_3L(3\text{-}Br\text{-}5\text{-}Cl\text{-}Sal)_2]\cdot 2MeCN$ ($5\cdot 2MeCN$). A few single crystals of this complex are isolated from **2** by exactly the same procedure as that described for $\mathbf{4}\cdot 2MeCN$.

---

[12] For example, see:(a) Fondo, M.; García-Deibe, A. M.; Bermejo, M. R.; Sanmartín, J.; Llamas-Saiz, A. L. *J. Chem. Soc., Dalton Trans.* **2002**, 4746–4750. (b) Fondo, M.; García-Deibe, A. M.; Ocampo, N.; Bermejo, M. R.; Sanmartín, J. *Dalton Trans.* **2004**, 2135–2141. (c) Fondo, M.; García-Deibe, A. M.; Corbella, M.; Ruiz, E.; Tercero, J.; Sanmartín, J.; Bermejo, M. R. *Inorg. Chem.* **2005**, *44*, 5011–5020. (d) Fondo, M.; Ocampo, N.; García-Deibe, A. M.; Vicente, R.; Corbella, M.; Bermejo, M. R.; Sanmartín, J. *Inorg. Chem.* **2006**, *45*, 255–262. (e) Fondo, M.; García-Deibe, A. M.; Ocampo, N.; Sanmartín, J.; Bermejo, M. R.; Oliveira, E.; Lodeiro, C. *New J. Chem.* **2008**, *32*, 247–257.

[$Cu_3L(OMe)_2$]·MeOH (6·MeOH). This complex is obtained as single crystals by the reaction of **3**·$3H_2O$ (0.053 g, 0.036 mmol) with $NMe_4OH·5H_2O$ (0.013 g, 0.072 mmol), following exactly the same procedure as that described for **4**·2MeCN. Yield: 0.044 g (89%). Mp: >300 °C. Calcd for $C_{41}H_{42}Br_4Cl_4Cu_3N_6O_7$ (1382.87): C, 35.57; H, 3.04; N, 6.07. Found: C, 35.27; H, 2.89; N, 6.04. MS (ES^+): *m*/*z* 1305.4 [$Cu_3L(OH)$]$^+$, 1319.4 [$Cu_3L(OMe)$]$^+$. IR (KBr, ν/cm^{-1}): 1633 (C=N).

X-ray Structure Determinations. Single crystals of **2**·2MeCN·2MeOH, **4**·2MeCN, **5**·2MeCN, and **6**·MeOH were obtained as detailed above. Diffraction data were collected at 120 K (**2**·2MeCN·2MeOH) or 100 K (**4**·2MeCN, **5**·2MeCN, and **6**·MeOH), using a Bruker SMART CCD-1000 diffractometer employing graphite monochromatic Mo-Kα radiation (λ = 0.710 73 Å). No significant decays were observed, and data were corrected for Lorentz and polarization effects. Multiscan absorption corrections were applied using *SADABS*.[13] The structures were solved by standard direct methods, employing *SIR-92*,[14] and refined by Fourier techniques based on F^2 using *SHELXL-97*.[15] Non-hydrogen atoms were anisotropically refined. Hydrogen atoms of organic groups were included at geometrically calculated positions, with thermal parameters derived from the parent atoms. Hydrogen atoms attached to water molecules or to groups suitable for forming hydrogen bonds could be located on Fourier maps, fixed and given isotropic displacement parameters of 0.08 Å^2 or depending on the parent atoms.

Magnetic Measurements. Magnetic susceptibility measurements for powder crystalline samples of **2**, **3**·$3H_2O$, and **6**·MeOH were carried out at the Unitat de Mesures Magnètiques of Universitat de Barcelona with a Quantum Design SQUID MPMS-XL susceptometer. The magnetic susceptibility data were recorded in the 2−300 K temperature range under magnetic fields of 400 G (2−30 K) and 7000 G (2−300 K) for **2** and of 500 G (2−30 K) and 10 000 G (2−300 K) for **3**·$3H_2O$ and **6**·MeOH. Diamagnetic corrections were estimated from Pascal's tables. The agreement factor is based on the function $R = \sum(\chi_M T_{exp} - \chi_M T_{cal})^2/\sum(\chi_M T_{exp})^2$. Magnetic fields ranging from 0 to 50 000 G were used for magnetization measurements at 2 K.

Results and Discussion

Ligand Synthesis. The new tricompartmental Schiff base H_4L can be prepared by direct interaction between 3-Br-5-Cl-Sal and pentaethylenehexamine, as summarized in Scheme 2. Characterization of the ligand by elemental analysis, ES mass spectrometry, and IR and ^1H NMR spectroscopies agrees with the isolation of H_4L with high purity, as well as with its stability in solution. Thus, the IR spectrum shows two main bands at 1636 and 3437 cm^{-1}, which can be assigned to the asymmetric stretching frequencies of the C=N and phenol OH groups,[16] respectively. The mass spectrum of the ligand is in agreement with the one expected: it shows a peak of 100% intensity at *m*/*z* 1102.8, corresponding to the molecular fragment [H_5L]$^+$. The stability and purity of the ligand in solution is also supported by the ^1H NMR spectrum, recorded in DMSO-d_6 as the solvent (Figure S1 in the Supporting Information). This spectrum shows a unique set of signals that are in complete accordance with the predictable ones.

Metal Complex Syntheses and Reactivity. The reactions of H_4L with 3 equiv of zinc(II), nickel(II), and copper(II) acetate in methanol/acetonitrile yield the trinuclear complexes **1**·H_2O, **2**·2MeCN·2MeOH, and **3**·$3H_2O$, respectively. **2**·2MeCN·2MeOH was isolated as single crystals, and it loses the solvate molecules upon drying to give **2**.

The stability and reactivity of **1**·H_2O to **3**·$3H_2O$ in a basic medium was investigated. Accordingly, the acetate complexes were treated with 2 equiv of $NMe_4OH·5H_2O$ in air, and the reaction pattern seems to depend on the metal ion. Thus, the reaction of **1**·H_2O and **2** with the base in methanol/acetonitrile gives rise to solutions that, upon slow concentration (4 weeks), generate a few single crystals of **4**·2MeCN and **5**·2MeCN, respectively. Both compounds contain two 3-Br-5-Cl-Sal$^-$ exogenous donors that originate from the partial hydrolysis of the H_4L ligand, presumably assisted by the metal ions. The reaction of **3**·$3H_2O$ with $NMe_4OH·5H_2O$ visibly differs from that of **1**·H_2O and **2**, and it leads to the methanolate complex **6**·MeOH, in the form of single crystals. Therefore, no appreciable hydrolysis of the ligand was observed in this case, where the exchange of the acetate ligands of **3** by methanolate donors in **6** takes place. It should be noted that the reactivity of these complexes in a basic medium clearly diverges from that of dinuclear complexes with comparable dicompartmental ligands (Scheme 1): most of the published complexes with these related donors fix atmospheric carbon dioxide in the presence of a base[12a−12d] while this ability is not shown by **1** to **3**. This lack of activity toward carbon dioxide absorption can probably be due to the presence of two electron-withdrawing substituents in the aromatic rings of H_4L, which decreases the electron-donor character of the ligand.

Complexes **2**·2MeCN·2MeOH, **4**·2MeCN, **5**·2MeCN, and **6**·MeOH were crystallographically characterized. The small quantity of crystals obtained for **4**·2MeCN and **5**·2MeCN prevented its further characterization. Complexes **1**·H_2O, **2**, **3**·$3H_2O$, and **6**·MeOH were additionally studied by spectroscopic, spectrometric, and analytical methods, and **2**, **3**·$3H_2O$, and **6**·MeOH were also magnetically analyzed.

The IR spectra of all of the compounds contain a sharp band at ca. 1630 cm^{-1}, in agreement with coordination of the Schiff base to the metal ions through the imine nitrogen atoms. The ES mass spectra of the acetate complexes show peaks with mass and isotopic distribution patterns related to the fragments [$M_3L(OH)$]$^+$ and [$M_3L(OAc)$]$^+$. The formation of fragments containing oxygen from compounds with bridging oxygen donor ligands is well documented in the literature[17,18] and, therefore, the presence of the [$M_3L(OH)$]$^+$ peak seems

---

(13) a *SADABS, Area-Detector Absorption Correction*; Siemens Industrial Automation Inc.: Madison, WI, 1996. (b) Blessing, R. H. Acta Crystallogr. 1995, A51, 33–38.

(14) Altomare, A.; Cascarano, G.; Giacovazzo, C.; Guagliardi, A. SIR92 A program for crystal structure solution. *J. Appl. Crystallogr.* 1993, 26, 343−350.

(15) Sheldrick, G. M. *SHELX97 Programs for Crystal Structure Analysis*; Institüt für Anorganische Chemie der Universität: Göttingen, Germany, 1998.

(16) Nakamoto, K. *Infrared and Raman Spectra of Inorganic and Coordination Compounds*, 5th ed.; John Wiley and Sons: New York, 1997.

(17) Andersen, U. N.; McKenzie, C. J.; Bojensen, G. *Inorg. Chem.* **1995**, *34*, 1435–1439.

(18) McKenzie, C. J.; Dalgard, P. *J. Mass Spectrom.* **1999**, *34*, 1033–1039.

Table 1. Crystal Data and Structure Refinement Parameters for **2**·2MeCN·2MeOH, **4**·2MeCN, **5**·2MeCN and **6**·MeOH

	2·2MeCN·2MeOH	**4**·2MeCN	**5**·2MeCN	**6**·MeOH
empirical formula	$C_{50}H_{60}Br_4Cl_4N_8Ni_3O_{12}$	$C_{56}H_{44}Br_6Cl_6N_8O_8Zn_3$	$C_{56}H_{44}Br_6Cl_6N_8Ni_3O_8$	$C_{41}H_{42}Br_4Cl_4Cu_3N_6O_7$
fw	1602.63	1845.26	1825.28	1382.87
cryst syst	monoclinic	monoclinic	monoclinic	triclinic
space group	$C2/c$	$P2_1/c$	$P2_1/c$	$P\bar{1}$
T (K)	120(2)	100(2)	100(2)	100(2)
a (Å)	23.584(4)	15.1332(13)	15.160(4)	11.698(2)
b (Å)	12.729(2)	13.9245(13)	13.823(4)	15.583(3)
c (Å)	19.937(3)	30.334(3)	30.307(8)	16.119(3)
α (deg)	90	90	90	62.348(2)
β (deg)	93.538(3)	99.398(2)	99.503(5)	72.600(3)
γ (deg)	90	90	90	75.990(3)
V (Å^3)	5973.9(17)	6306.2(10)	6264(3)	2465.0(8)
Z	4	4	4	2
μ (mm^{-1})	3.856	5.248	5.037	4.795
reflns collected	34261	47517	51019	28337
indep reflns	6125 (R_{int} = 0.0451)	10782 (R_{int} = 0.0461)	12307 (R_{int} = 0.0743)	10103 (R_{int} = 0.0440)
data/restraints/param	6125/0/369	10782/0/786	12307/0/786	10103/0/598
final R index [$I > 2\sigma(I)$]	R1 = 0.0492, wR2 = 0.0924	R1 = 0.0454, wR2 = 0.0781	R1 = 0.0453, wR2 = 0.0937	R1 = 0.0534, wR2 = 0.1262
R index [all data]	R1 = 0.1239, wR2 = 0.1275	R1 = 0.1129, wR2 = 0.0997	R1 = 0.0904, wR2 = 0.1120	R1 = 0.1041, wR2 = 0.1435

to indicate that the acetate ligands act as bridges. The mass spectrum for **6**·MeOH shows two peaks at m/z 1305.4 and 1319.4, corresponding to the fragments $[Cu_3L(OH)]^+$ and $[Cu_3L(OMe)]^+$, respectively. Thus, the mass spectrometry corroborates the trinuclear nature of all of the complexes in solution and suggests coordination of the acetate or methanolate exogenous ligands to the metal atoms in a bridging mode.

Moreover, the ^{1}H NMR spectrum of **1**·H_2O was recorded in DMSO-d_6 as the solvent. The spectrum is also in accordance with the proposed formulation for **1**·H_2O and with its high purity. In addition to the typical imine (8.36 ppm) and imidazolidine (4.01 and 4.61 ppm) peaks, the nonexistence of signals above 8.5 ppm is remarkable, which is in agreement with the lack of phenol hydrogen atoms and, therefore, with the tetraanionic character of the ligand in the complex. Besides, one singlet (6H) at 1.80 ppm, which is absent in the free Schiff base, indicates the presence and coordination of two exogenous acetate donors.[12a,12b,19]

Description of the Crystal Structures. Single crystals of **2**·2MeCN·2MeOH, **4**·2MeCN, **5**·2MeCN and **6**·MeOH, suitable for X-ray structure determination, were obtained as detailed above. Crystallographic experimental details are collected in Table 1.

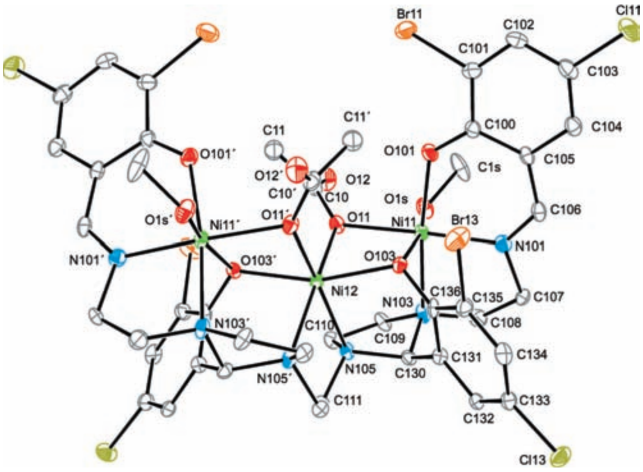

Figure 1. ORTEP view of the crystal structure of **2**. Hydrogen atoms are omitted for clarity. Ellipsoids are drawn at 40% probability.

Table 2. Selected Bond Lengths (Å) and Angles (deg) for **2**·2MeCN·2MeOH[a]

Ni11−O101	1.995(5)	Ni12−O103	2.015(4)
Ni11−N101	1.996(6)	Ni12−O11	2.126(5)
Ni11−O11	2.062(5)	Ni12−N105	2.270(6)
Ni11−O103	2.118(5)		
Ni11−N103	2.119(6)		
Ni11−O1S	2.130(5)	Ni11···Ni12	3.178(5)
N101−Ni11−O11	174.1(2)	O103′−Ni12−O103	162.7(3)
O101−Ni11−N103	171.1(2)	O11−Ni12−N105′	165.85(19)
O103−Ni11−O1S	167.65(19)		
Ni11−O11−Ni12	98.69(19)	Ni11−O103−Ni12	100.49(19)

[a] ′ = −x, y, −z + $^3/_2$.

2·2MeCN·2MeOH. An ORTEP view of **2** is shown in Figure 1, and the main distances and angles are listed in Table 2. The crystallographic asymmetric unit of **2**·2MeCN·2MeOH contains, in addition to an acetonitrile and a methanol molecule as solvates, half of a $[Ni_3L(OAc)_2(MeOH)_2]$ trinuclear complex, with the other half molecule being generated by a C_2 axis (symmetry operation x, y, $-z + {}^3/_2$) that goes by the Ni12 atom.

The trinuclear complex, of perfect C_{2v} symmetry, contains a tetraanionic L^{4-} ligand, which behaves as tricompartmental and decadendate, leading to a trinuclear array with a Ni11···Ni12···Ni11′ angle of 141.80°. Thus, the ligand uses each one of its external N_2O cavities (N_{imine}, N_{amine}, and O_{phenol}) to allocate a nickel(II) ion and the central N_2O_2 (N_{amine} and O_{phenol}) pocket to link a third metal atom. Besides, the phenol oxygen atoms of the central compartment (O103 and O103′) act as bridges between Ni12 and Ni11 (or Ni11′). The coordination spheres of the metal ions are completed by two acetate exogenous ligands, linked as bridging monodentate, and by two methanol molecules, joined to Ni11 and Ni11′. As a result, the nickel ions are in N_2O_4 environments, with

---

(19) Beattie, J. K.; Klepelko, J. A.; Masters, A. F.; Turner, P. *Polyhedron* **2003**, *22*, 947–965.

distorted octahedral geometries, and triply bridged ($NCN_{imidazolidine}$, O_{phenol}, and $O_{acetate}$), with Ni···Ni distances of ca. 3.18 Å (Figure 2). This situation leads to $Ni-O_{acetate}-Ni$ angles (98.69°) more acute than the $Ni-O_{phenol}-Ni$ (100.49°) ones, with distances and angles that are typical of nickel(II) in this distorted environment.[12c,20]

Finally, it should be noted that the spatial disposition of the Schiff base induces chirality, although the crystals are racemic mixtures, because both enantiomers are present in the unit cell at 50%.

4·2MeCN and 5·2MeCN. The crystal structures of both complexes are quite similar, and they will be discussed together. ORTEP views of **4** and **5** are shown in Figures 3 and 4, respectively, and the main distances and angles are given in Tables 3 and 4.

Both compounds contain $[M_3L(3\text{-Br-5-Cl-Sal})_2]$ molecules in the unit cell and acetonitrile as the solvate. In these trinuclear complexes, the Schiff base behaves as trinucleating and decadendate, in a manner similar to that described for **2**: it allocates two metal ions in its external N_2O compartments and a third metal atom in the central N_2O_2 cavity, leading to trinuclear arrays with M11···M12···M13 angles of 125.18° and 128.41° for **4** and **5**, respectively. Moreover, the central phenol oxygen atoms (O103 and O104) also act as bridges in the case of **5**, but it is remarkable that the ligand seems to behave as an asymmetric donor in **4**: it makes use of one of its central phenol oxygen atoms (O103) to bridge Zn11 and Zn12, while the second one (O104) should really be considered as a terminal donor, given the long distance Zn13···O104 [2.448(5) Å]. This distance maybe should be best described as a secondary intramolecular interaction or a semibond, as previously published.[21]

In both **4** and **5**, the coordination spheres of the metal ions are completed by two 3-Br-5-Cl-Sal$^-$ exogenous ligands, which act in a $\mu-\eta^1:\eta^2$-O,O′ fashion between adjacent metal ions: the phenol oxygen atom (O*X*0, X = 1 or 2) is bound to one external metal ion while the carbonyl oxygen atom (O*X*1) bridges two metal centers. As a result, the nickel centers are in distorted-octahedral N_2O_4 environments in **5** while, if the semibond is ignored, the zinc ions show different coordination numbers in **4**. Accordingly, two zinc ions (Zn11 and Zn12) are N_2O_4 coordinated, with distorted octahedral geometries, while the third metal ion (Zn13) is in a N_2O_3 environment, with a τ paramater[22] (0.08) that suggests a slightly distorted square-pyramidal geometry. In this pyramid, the phenol oxygen atom O20 occupies the apical site.

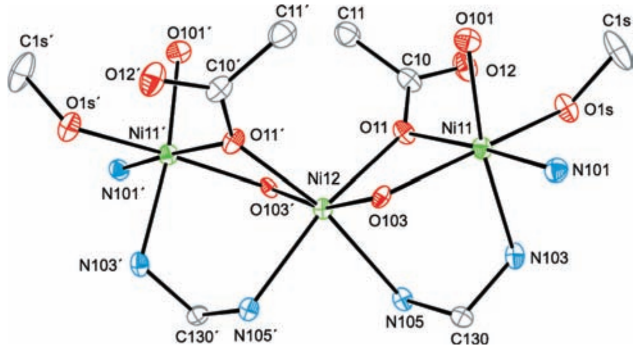

Figure 2. Core of **2** showing the bridging ligands between nickel atoms.

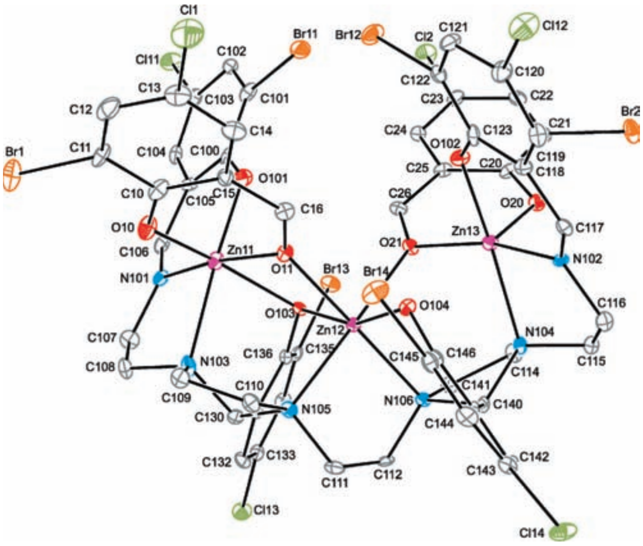

Figure 3. ORTEP view of the crystal structure of **4**. Hydrogen atoms are omitted for clarity. Ellipsoids are drawn at 40% probability.

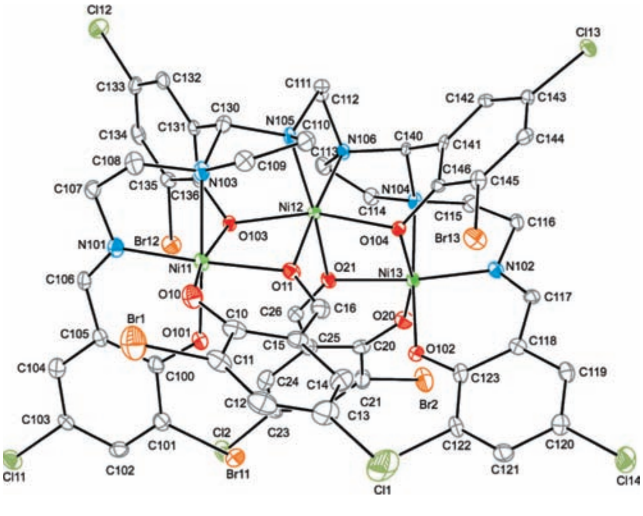

Figure 4. ORTEP view of the crystal structure of **5**. Hydrogen atoms are omitted for clarity. Ellipsoids are drawn at 40% probability.

The discussed features lead to dissimilar numbers of bridges between adjacent M···M atoms. Thus, in **5**, the nickel ions are triply bridged ($NCN_{imidazolidine}$, O_{phenol}, and $O_{carbonyl}$), with Ni···Ni distances of ca. 3.1 Å. In the case of **4**, Zn11···Zn12 are also triply bridged (an $NCN_{imidazolidine}$ and two oxygen bridges) while Zn12··· Zn13 are doubly bridged (an $NCN_{imidazolidine}$ and one

---

(20) Fondo, M.; García-Deibe, A. M.; Ocampo, N.; Sanmartín, J.; Bermejo, M. R.; Llamas-Saiz, A. M. *Dalton Trans* **2006**, 4260–4270.

(20) Fondo, M.; García-Deibe, A. M.; Ocampo, N.; Sanmartín, J.; Bermejo, M. R.; Llamas-Saiz, A. M. *Dalton Trans* **2006**, 4260–4270.

(21) (a) Bernarducci, E. E.; Bharadwaj, P. K.; Lalancette, R. A.; Krogh-Jespersen, K.; Potenza, J. A.; Schugar, H. J. *Inorg. Chem.* **1983**, *22*, 3911–3920. (b) Tyson, T. A.; Hodgson, K. O.; Hedman, B.; Clark, G. R. *Acta Crystallogr.* **1990**, *C46*, 1638–1640. (c) Garnovskii, A. D.; Antsishkina, A. S.; Vasil'chenko, I. S.; Sergienko, V. S.; Kochin, S. G.; Nivorozhkin, A. L.; Misteryukov, A. E.; Uraev, A. I.; Garnovskii, D. A. *Russ. J. Inorg. Chem.* **1995**, *40*, 67–70. (d) Das, S.; Bharadwaj, P. K. *Cryst. Growth Des.* **2006**, *6*, 187–192.

(22) Addison, A. W.; Rao, T. N.; Reedijk, J.; Van Rijk, J.; Verschoor, G. C. *J. Chem. Soc., Dalton Trans.* **1984**, 1349–1356.

Table 3. Selected Bond Lengths (Å) and Angles (deg) for **4**·MeCN

Zn11−O101	1.958(5)	Zn13−O102	1.972(5)
Zn11−N101	2.020(6)	Zn13−N102	1.995(6)
Zn11−O10	2.055(5)	Zn13−O21	2.048(5)
Zn11−O11	2.073(5)	Zn13−O20	2.074(5)
Zn11−O103	2.234(5)	Zn13−N104	2.261(6)
Zn11−N103	2.278(6)		
Zn12−O104	2.008(5)		
Zn12−O103	2.028(5)		
Zn12−O11	2.160(5)	Zn11···Zn12	3.191(6)
Zn12−O21	2.161(5)	Zn12···Zn13	3.252(6)
Zn12−N106	2.182(6)		
Zn12−N105	2.196(6)		
O101−Zn11−N103	173.0(2)	N102−Zn13−O21	169.7(2)
N101−Zn11−O11	171.4(2)	N102−Zn13−O21	164.6(2)
O10−Zn11−O103	161.6(2)	Zn11−O11−Zn12	97.8(2)
O11−Zn12−N106	171.4(2)	Zn12−O21−Zn13	101.2(2)
O21−Zn12−N105	170.7(2)	Zn11−O103−Zn12	96.9(2)
O104−Zn12−O103	160.5(2)		

Table 4. Selected Bond Lengths (Å) and Angles (deg) for **5**·MeCN

Ni11−O101	1.962(4)	Ni13−N102	1.961(5)
Ni11−N101	1.969(5)	Ni13−O102	1.973(4)
Ni11−O11	2.006(4)	Ni13−O21	1.989(4)
Ni11−O10	2.032(4)	Ni13−O20	2.081(4)
Ni11−N103	2.141(5)	Ni13−N104	2.151(5)
Ni11−O103	2.146(4)	Ni13−O104	2.225(4)
Ni12−O104	2.013(4)		
Ni12−O103	2.028(4)		
Ni12−O21	2.067(4)	Ni11···Ni12	3.080(5)
Ni12−O11	2.075(4)	Ni12···Ni13	3.107(5)
Ni12−N106	2.133(5)		
Ni12−N105	2.140(5)		
O101−Ni11−N103	177.9(2)	O102−Ni13−N104	175.8(2)
N101−Ni11−O11	174.5(2)	N102−Ni13−O21	171.1(2)
O10−Ni11−O103	167.3(2)	O20−Ni13−O104	165.3(2)
O11−Ni12−N106	173.3(2)	Ni11−O11−Ni12	98.0(2)
O21−Ni12−N105	173.1(2)	Ni12−O21−Ni13	100.0(2)
O104−Ni12−O103	162.3(2)	Ni11−O103−Ni13	95.0(2)
		Ni13−O104−Ni12	94.1(2)

oxygen bridge), which gives rise to Zn11···Zn12 and Zn12···Zn13 distances of 3.191(6) and 3.252(6) Å, respectively.

Also, in these cases, the complexes cannot be superposed on their mirror images but, once more, the unit cell contains both enantiomers at 50%. The optical isomerism for these compounds is based not only on the disposition of the trinucleating ligand but also on the asymmetric coordination mode of the salicyaldehydate exogenous donor, a situation that has been addressed for complexes of related dicompartmental donors as well.[23]

6·MeOH. An ORTEP diagram of **6** is shown in Figure 5, and the main distances and angles are listed in Table 5.

The asymmetric unit of this crystal contains [Cu$_3$L(OMe)$_2$] molecules and methanol as the solvate. The structure of [Cu$_3$L(OMe)$_2$] is similar to that described for **2**, **4**, and **5**, with some notable differences. Thus, the L^{4-} ligand also allocates three copper(II) ions, with a Cu11···Cu12···Cu13 angle of 129.44°, but, in this case, the Schiff base behaves as an N$_2$O$_2$ + N$_2$ + N$_2$O$_2$ donor. Accordingly, Cu12 only binds to both nitrogen atoms of the central cavity (N105 and N106) because the Cu12···O103 and Cu12···O104 distances [2.363(4) and 2.313(4) Å, respectively] seem to indicate that they are second intramolecular interactions. The coordination spheres of the metal atoms are completed by two methanolate anions, acting as bridges between adjacent copper ions. Therefore, the metal atoms are only doubly bridged (an NCN$_{\text{imidazolidine}}$ and one oxygen bridge), with Cu···Cu distances close to 3.1 Å and Cu−O−Cu angles of ca. 107°. As a result, Cu11 and Cu13 are N$_2$O$_3$-coordinated, with τ parameters (0.047 for Cu11 and 0.027 for Cu13) that indicate a slightly distorted square-pyramidal geometry, where O103 and O104 occupy the apical sites. Cu12 is N$_2$O$_2$-coordinated, if the semicoordination bonds are not taken into account, and it is in an almost square-planar environment (maximum deviation of any atom from the mean calculated plane 0.048 Å, with the copper atom sitting on the plane).

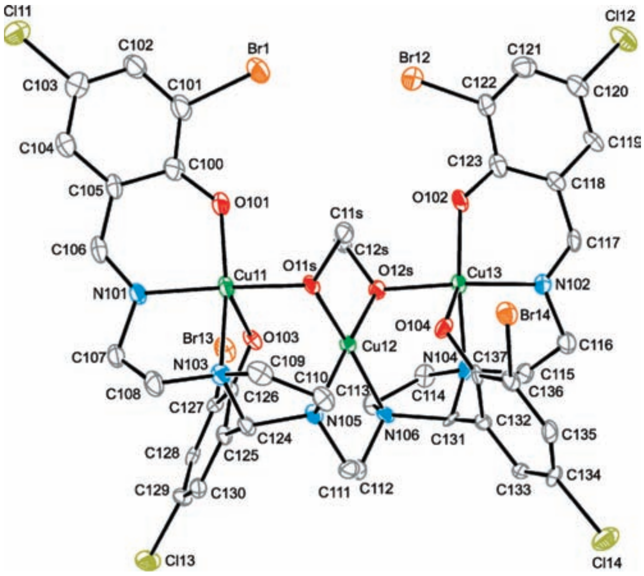

Figure 5. ORTEP view of the crystal structure of **6**. Hydrogen atoms are omitted for clarity. Ellipsoids are drawn at 40% probability.

Last, it is worth mentioning that this complex is chiral as well but, once again, it crystallizes as a racemic mixture.

As an end result of the crystallographic studies, it should be emphasized that the Schiff base ligand always behaves as tetraanionic, tricompartmental, and decadendate, invariably providing two NCN bridges between the three adjacent coordinated ions. More interestingly, these studies demonstrate that the L^{4-} donor does not satisfy the stereochemical requirements of the metal ions, with the coordination spheres being completed by exogenous donors. These donors seem to be labile coordination positions, which can be easily replaced. Therefore, these M$_3$ complexes fit the essential prerequisites to be used as building blocks in the construction of complexes of higher-nuclearity and/or coordination polymers. Accordingly, L^{4-} plugs most of the coordination sites of the metal ions but leaves some coordination vacancies, which could be filled by appropriate bridging connectors, so expanding the trinuclear nodes. Moreover, it is worth noting that the ligand induces chirality per se in all of the complexes, regardless of the symmetry or asymmetry of the exogenous coordinated anions. Nevertheless, in all these cases both enantiomers are present at 50% in the unit cell, thus producing racemic mixtures and not

---

[23] Paital, A. R.; Ribas, J.; Barrios, L. A.; Aromí, G.; Ray, D. *Dalton Trans* **2009**, 256–258.

Table 5. Selected Bond Lengths (Å) and Angles (deg) for **6**·MeOH

Cu11−O11S	1.910(4)	Cu13−O12S	1.893(4)	Cu12−O11S	1.937(4)
Cu11−O101	1.930(5)	Cu13−O102	1.927(5)	Cu12−O12S	1.948(4)
Cu11−N101	1.948(5)	Cu13−N102	1.946(5)	Cu12−N105	2.119(5)
Cu11−N103	2.174(5)	Cu13−N104	2.180(5)	Cu12−N106	2.139(6)
Cu11−O103	2.205(5)	Cu13−O104	2.207(4)		
Cu11···Cu12	3.1052(14)	Cu12···Cu13	3.0784(14)		
O11S−Cu11−N101	166.4(2)	O12S−Cu13−N102	166.0(2)	O12S−Cu12−N105	173.16(19)
O101−Cu11−N103	163.6(2)	O102−Cu13−N104	164.4(2)	O11S−Cu12−N106	172.3(2)
		Cu11−O11s-Cu12	107.7(2)	Cu12−O12s-Cu13	106.5(2)

optically active species. In spite of this, the mentioned features (undoubtedly trinucleating character, generation of trinuclear blocks, and induction of chirality) make H_4L a promisingly useful ligand in such outstanding research fields as molecular magnetism, supramolecular chemistry, or the search for optically active compounds.

Magnetic Studies. The magnetic properties of **2**, **3**·$3H_2O$, and **6**·MeOH have been investigated in the 2−300 K temperature range. A plot of $\chi_M T$ vs T for **2** is shown in Figure 6, where it can be seen that the $\chi_M T$ product at 300 K is 3.37 $\text{cm}^3\ \text{mol}^{-1}$ K, a value than can be considered as typical for three uncoupled nickel(II) ions with $g > 2.0$. This value remains almost constant between 300 and 100 K, then increases upon cooling to reach a maximum at 6 K (4.22 $\text{cm}^3\ \text{mol}^{-1}$ K), and finally decreases with decreasing temperature. Thus, the observed behavior indicates an intramolecular ferromagnetic coupling, with the decrease in $\chi_M T$ at low temperature being attributed to either intermolecular antiferromagnetic interactions or the effect of the zero-field splitting (ZFS) of the ground state. Magnetization measurements at 2 K also suggest a predominant ferromagnetic coupling. The $M/N\beta$ vs H curve tends to 5 at 50 000 G, indicating a nonisolated $S = 3$ ground state and/or the presence of ZFS.

The susceptibility curve was treated with the *MAGPACK* program,[24] where the exchange spin Hamiltonian is expressed as $H = -2\sum J_{ij}S_iS_j$. As previously discussed, the structural data reveal that **2** is a trinuclear complex with a triple bis(μ-O)-μ-NCN bridge between adjacent metal ions (Scheme 3). Because the molecule presents a C_2 axis that goes by Ni12, the bridges between adjacent nickel atoms are exactly equal. Besides, the possible magnetic interaction between the external metal atoms, promoted by the methylene chain of the amine residue, must be negligible because of the long distance between both metal centers. Thus, a $1 - J$ model was chosen in order to reproduce the magnetic behavior of **2**. Moreover, it should be noted that the crystallographic data do not show significant short intermolecular interactions between trinuclear molecules. Accordingly, with these considerations in mind, the fit with the *MAGPACK* program was performed with the mentioned $1 - J$ model and with introduction of the D_{Ni} parameter, with the aim of accounting for the decrease in $\chi_M T$ at low temperature. The best fit gives the values $2J = 2.52\ \text{cm}^1$, $g = 2.08$, $|D_{\text{Ni}}| = 6.07\ \text{cm}^{-1}$, and TIP $= 1.59 \times 10^{-4}\ \text{cm}^3\ \text{mol}^{-1}$ ($R = 6.29 \times 10^{-4}$), which yields an $S = 3$ ground state, in agreement with the magnetization measurements at 2 K.

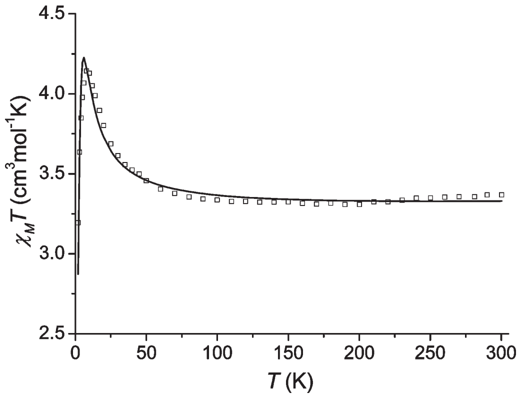

Figure 6. Plot of $\chi_M T$ vs T for **2**: scattered points, experimental results; dashed line, best fit.

The reliability of the obtained variables was analyzed. $2J$, as mentioned, denotes the magnetic coupling through the triple bis(μ-oxo)-μ-NCN bridge, with an average Ni−O−Ni angle of 99.6°, and its value is in complete agreement with the previous data reported in the literature for this class of a superexchange magnetic pathway.[12d,20,25] Moreover, the $|D_{\text{Ni}}|$ parameter is in the range of the one expected for a nickel(II) ion in a distorted-octahedral environment.[26]

The $\chi_M T$ vs T graphs for **3**·$3H_2O$ and **6**·MeOH (Figures 7 and 8, respectively) are very similar. In both cases, the $\chi_M T$ product at 300 K (1.45 $\text{cm}^3\ \text{mol}^{-1}$K for **3**·$3H_2O$ and 1.41 $\text{cm}^3\ \text{mol}^{-1}$K for **6**·MeOH) is close to that expected for three magnetically isolated spin doublets. This value gradually decreases upon cooling, suggesting an overall intramolecular antiferromagnetic coupling. The structural analysis for **6**·MeOH has shown that the adjacent copper ions (with Sqp or Sp geometry) are doubly bridged by an oxygen atom of a methanolate donor and by the $\text{NCN}_{\text{imidazolidine}}$ fragment of the Schiff base and that both bridges are in the basal plane. Besides, the Cu−O and Cu−N distances, as well as the Cu−O−Cu angles of adjacent bridges, are quite similar. Although the crystal structure for **3**·$3H_2O$ could not be solved, the comparison of **2**·2MeCN·2MeOH and **5**·2MeCN shows that the replacement of the exogenous ligands does not significantly modify the structure of the complex. Accordingly, **3**·$3H_2O$ should be structurally similar to **6**·MeOH. Therefore, a $1 - J$ model (Scheme 4) should be

---

[24] (a) Borrás-Almenar, J. J.; Clemente, J. M.; Coronado, E.; Tsukerblat, B. S. *Inorg. Chem.* **1999**, *38*, 6081–6088. (b) Borrás-Almenar, J. J.; Clemente, J. M.; Coronado, E.; Tsukerblat, B. S. *J. Comput. Chem.* **2001**, *22*, 985–991.

[25] (a) Paital, A. R.; Mikuriya, M.; Ray, D. *Eur. J. Inorg. Chem.* **2007**, 5360–5369. (b) Paital, A. R.; Wong, W. T.; Aromí, G.; Ray, D. *Inorg. Chem.* **2007**, *46*, 5727–5733.

[26] Boca, R. *Coord. Chem. Rev.* **2004**, *248*, 757–815.

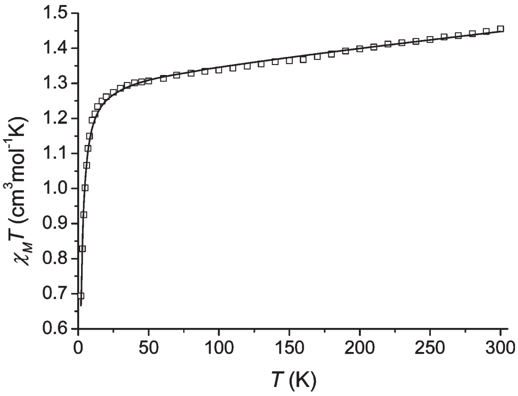

Figure 7. Plot of $\chi_M T$ vs T for **3**·3H_2O: scattered points, experimental results; dashed line, best fit.

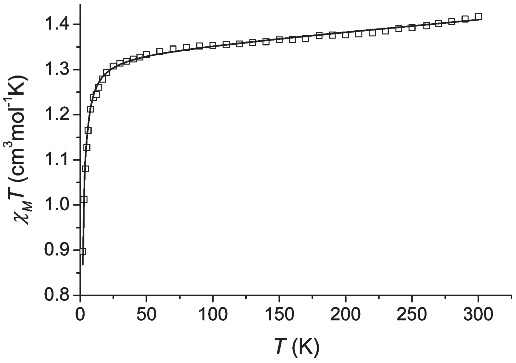

Figure 8. Plot of $\chi_M T$ vs T for **6**·MeOH: scattered points, experimental results; dashed line, best fit.

Scheme 3

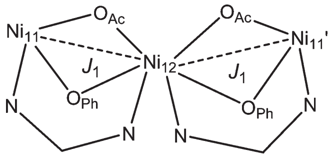

Scheme 4

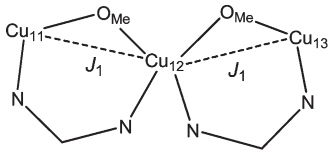

enough to explain the magnetic behavior in both cases. The best fit of the data using the *MAGPACK* program with this model ($H = 2\sum J_{ij}S_iS_j$) yields the following values: $2J = -2.22$ cm^{-1}, $g = 2.16$, and TIP = 4.63×10^{-4} cm^3 mol^{-1} ($R = 6.42 \times 10^5$) for **3**·3H_2O and $2J = -1.44$ cm^{-1}, $g = 2.18$, and TIP = 2.63×10^{-4} cm^3 mol^{-1} ($R = 3.38 \times 10^5$) for **6**·MeOH, which entails an $S = {}^1/_2$ ground state in both cases. Thus, the magnetic studies also agree with the trinuclear character of the X-ray crystallographically unresolved complex **3**·3H_2O.

The weak antiferromagnetic coupling observed for these complexes is unexpected. In fact, this research group has previously demonstrated by means of density functional theory (DFT) calculations that the apparently anomalous ferromagnetic behavior of $[(Cu_2L^1)_2(CO_3)]\cdot 8H_2O$[12c] ($H_3L^1 = H_3L^x$ in Scheme 1, where R = H) is due to the countercomplementary effect of the $NCN_{imidazolidine}$ and oxo bridges that mediate the magnetic coupling, a result further supported by additional DFT studies on a similar perchlorate Cu_4 cluster.[27] Moreover, as far as we know, all of the copper complexes where one $NCN_{imidazolidine}$ and one oxygen bridge constitute the superexchange pathway are ferromagnetic.[12c,27,28] For this kind of complex, the magnitude of the magnetic interaction depends on the Cu−O−Cu angle and the angle between the basal planes of the polyhedra (θ).[28c] Thus, the Cu−O−Cu angles of ca. 107° and the θ values close to 60° (θ for basal planes about Cu11 and Cu12 of 61.20° and about Cu12 and Cu13 of 62.02°) should induce a quite strong ferromagnetic coupling.[28c] Finally, it should be mentioned that, as far as we know, all of the copper complexes containing an $NCN_{imidazolidine}$ bridge are ferromagnetic, except two noticeable exceptions.[29]

Consequently, some attempts were made in order to understand the weak antiferromagnetism of the samples, especially of the crystallographically solved **6**·MeOH. Accordingly, extended Hückel calculations with the crystallographic coordinates of **6** were carried out with the *CACAO* program.[30] The frontier orbitals for **6** are depicted in Figure 9, and from this study, some conclusions can be drawn. First of all, this calculation confirms some previous assumptions proposed on the basis of the crystallographic data. In this way, the study evidences that O103 and O104 are terminal donors and do not bind to Cu12. Therefore, as stated before, only the methanolate and NCN bridges contribute to mediation of the magnetic coupling. More interestingly, the frontier molecular orbitals (MOs) are not very delocalized. Thus, the MO of lower energy (MO 130 in Figure 9) essentially results from a combination of the $d_{x^2-y^2}$ orbital of Cu12 and the p orbitals of N105, N106, O11s, and O12s, while MO 129 is mainly centered on the Cu11 and Cu13 metals an their donor atoms, with no participation of the Cu12 orbitals. Finally, the orbital of highest energy (MO 128 in Figure 9) is the most delocalized one. In spite of this, it shows a low contribution of the $d_{x^2-y^2}$ orbital of Cu12 (3%) and the p orbitals of N105 and N106 (2% each) compared with the participation of the magnetic orbitals of Cu11 (13%) and Cu13 (21%), as well as with the contribution of the p orbitals of the external nitrogen atoms of the imidazolidine rings (N103 and N104). As a result, it seems that the partaking of the imidazolidine bridge in the superexchange pathway is small, if not negligible, and that the magnetic coupling is mainly mediated by methanolate oxygen atoms. In spite of this useful information, with just one complex with such a particular shape of the frontier orbitals, it should be daring to venture a possible

---

(27) Paital, A. R.; Bertolasi, V.; Aromí, G.; Ribas-Ariño, J.; Ray, D. *Dalton Trans.* **2008**, 861–864.

(28) (a) Fondo, M.; García-Deibe, A. M.; Sanmartín, J.; Bermejo, M. R.; Lezama, L.; Rojo, T. *Eur. J. Inorg. Chem.* **2003**, 3703–3706. (b) Fondo, M.; García-Deibe, A. M.; Corbella, M.; Ribas, J.; Llamas-Saiz, A. L.; Bermejo, M. R.; Sanmartín, J. *Dalton Trans.* **2004**, 3503–3507. (c) Fondo, M.; Ocampo, N.; García-Deibe, A. M.; Corbella, M.; Bermejo, M. R.; Sanmartín, J. *Dalton Trans.* **2005**, 3785–3794.

(29) (a) Bera, M.; Wong, W. T.; Aromí, G.; Ray, D. *Eur. J. Inorg. Chem.* **2005**, 2526–2535. (b) Nanda, P. K.; Bera, M.; Aromí, G.; Ray, D. *Polyhedron* **2006**, *25*, 2791–2799.

(30) Mealli, C.; Proserpio, D. M. *J. Chem. Educ.* **1990**, *67*, 399–402.

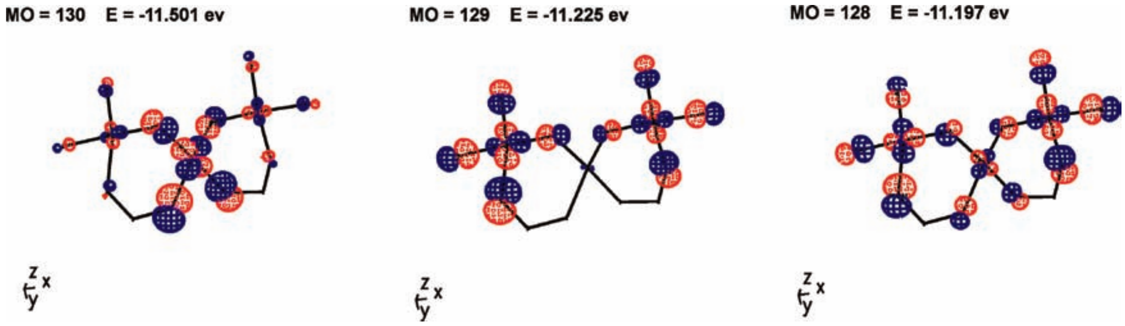

Figure 9. Frontier MOs for **6**.

explanation for the antiferromagnetism observed, and more examples of this kind of compound should be studied until magnetostructural correlations could be performed.

Conclusions

A new tricompartmental acyclic ligand, an uncommon class of donor, has been prepared with high yield and purity. This reacts with zinc, nickel, and copper acetate to generate the corresponding trinuclear acetate complexes **1**·H_2O, **2**, and **3**·$3H_2O$. The reactivity of these compounds in a basic medium was studied, and it seems to depend on the nature of the metal ion. Accordingly, **1**·H_2O and **2** undergo partial hydrolysis, generating **4**·2MeCN and **5**·2MeCN, respectively, while **3**·$3H_2O$ experiences a reaction of ligand exchange, yielding the methanolate complex **6**·MeOH. The crystallographic characterization of compounds **2**−**6** undoubtedly shows that the deprotonated L^{4-} ligand invariably acts as a tetraanionic, trinucleating, and decadendate donor. Interestingly, the ligand adopts such a spatial arrangement that it seems to induce chirality per se in its complexes. Also remarkable is the fact that L^{4-} does not fulfill the stereochemical requirements of the metal ions, and the coordination spheres of the metal atoms are completed by different exogenous donors, which are labile coordination positions. The lability of these coordination sites is evidenced by substitution of the acetate ligand in **1**−**3** by salicyladehydate or by methanolate donors in **4**−**6**. Thus, H_4L can give rise to trinuclear compounds that satisfy the necessary prerequisites to be used as nodes in the isolation of complexes of higher-nuclearity and/or coordination polymers: the polynucleating ligand blocks most of the coordination positions and leaves some free coordination sites, which could be occupied by suitable bridging donors, so expanding the trinuclear nodes. The magnetic characterization of **2**, **3**·$3H_2O$, and **6**·MeOH shows a weak magnetic coupling in all cases. As a summary, these topics (unquestionable trinucleating character, ability to produce trinuclear building blocks, and induction of chirality) turn H_4L into a kind of ligand with potential utility in many leading research fields (such as molecular magnetism, supramolecular chemistry, or the field of the optically active compounds). Therefore, this work lays the foundation for the more extensive study that the coordination chemistry of this type of donor deserves.

Acknowledgment. The authors thank Xunta de Galicia (PGIDIT04PXIC20902PN) for financial support.

Supporting Information Available: ^1H NMR spectrum for H_4L and X-ray crystallographic data in CIF format for **2**·2MeCN·2MeOH, **4**·2MeCN, **5**·2MeCN and **6**·MeOH. This material is available free of charge via the Internet at http://pubs.acs.org.